Available online at www.sciencedirect.com
ScienceDirect
Journal of Molecular Catalysis A: Chemical 283 (2008) 69–76
JOURNAL OF MOLECULAR CATALYSIS A: CHEMICAL
www.elsevier.com/locate/molcata

Direct synthesis of methanethiol from H_2S-rich syngas over sulfided Mo-based catalysts

Aiping Chen, Qi Wang, Qiaoling Li, Yingjuan Hao, Weiping Fang, Yiquan Yang *

College of Chemistry and Chemical Engineering, Xiamen University, Siming South Road No. 422, Xiamen 361005, PR China

Received 27 October 2007; received in revised form 11 December 2007; accepted 11 December 2007
Available online 23 December 2007

Abstract

The direct synthesis of methanethiol from H_2S-rich syngas was investigated over sulfided Mo-based catalysts supported on SiO_2. K-promoted Mo/SiO_2 catalysts exhibited a high activity for the synthesis of CH_3SH. The incorporation of cobalt into the $K–Mo/SiO_2$ catalyst increased the catalytic activity, but slightly decreased the selectivity to methanethiol. The selected catalysts were characterized by using X-ray diffraction (XRD), CO temperature-programmed desorption (CO-TPD), electron spin resonance (ESR), and X-ray photoelectron spectroscopy (XPS) techniques. The results showed that the potassium interacts with Mo component and increases the active sites for the CH_3SH synthesis by changing the concentration of Mo^{5+} species after sulfidation. A mechanism for the synthesis of CH_3SH was proposed.

Keywords: Methanethiol synthesis; Hydrogen sulfide; Syngas; Mo-based catalysts; Potassium; Cobalt; Hydrogenation

1. Introduction

Methanethiol (CH_3SH), also referred to as methyl mercaptan, is a colorless gas with a smell like rotten cabbage. Primarily, it is added as an odorant to propane and natural gas used as fuel. Methanethiol can further be used as an important intermediate in the production of organosulfur compounds, such as methionine, dimethyl sulfoxide, and dimethyl sulfone [1]. Industrially, it is synthesized in the gas phase from methanol and hydrogen sulfide over alumina-supported metal oxide catalysts at 300–500 °C and 0.1–2.5 MPa [1,2]. As expected, the $CH_3OH–H_2S$ route for the synthesis of methanethiol is an inefficient process, which proceeds via a methane steam reforming to syngas ($CO + H_2$) and the synthesis of methanol from syngas [3].

More than 20 years ago, Dow Chemical and Union Carbide scientists [4–7] reported that the molybdenum sulfide catalysts promoted with cobalt or alkali metals showed high activities for the synthesis of mixed alcohols from syngas. Such catalysts are claimed to be sulfur-tolerant and can be operated in a high sulfur-containing syngas (20–100 ppm). Subsequently, unsupported and supported Mo–S-based catalysts have been studied extensively for the synthesis of mixed alcohols [8–18]. However, the studies of the reactions of the syngas in the presence of high H_2S concentration are very sparse [3,19–26]. It is interesting since the mixed alcohols disappear and methanethiol become one of the dominant products when the concentration of H_2S in the syngas is over 1.6% [20,25]. Obviously, compared to the $CH_3OH–H_2S$ route, one-step synthesis of methanethiol from a simple feedstock such as H_2S-rich syngas (or $CO/H_2/H_2S$ mixtures) would be attractive and promising.

In this paper, the SiO_2-supported Mo-based catalysts were applied for the direct synthesis of methanethiol from H_2S-rich syngas. Potassium and cobalt were added as the promoters to SiO_2-supported Mo-based catalysts and the performance of the catalysts was investigated. To better understand the nature of the promoting effect of promoters, we performed X-ray diffraction (XRD), CO temperature-programmed desorption (CO-TPD), electron spin resonance (ESR), and X-ray photoelectron spectroscopy (XPS) characterizations for the selected catalysts. In the end, a possible mechanism for the synthesis of CH_3SH was proposed.

* Corresponding author. Tel.: +86 592 2186368; fax: +86 592 2186291.
E-mail address: yyiquan@xmu.edu.cn (Y. Yang).

1381-1169/$ – see front matter © 2007 Elsevier B.V. All rights reserved.
doi:10.1016/j.molcata.2007.12.014

2. Experimental

2.1. Catalyst preparation

Catalysts were prepared by the incipient wetness co-impregnation method. Inert SiO_2 (commercial sample, $S_{BET} = 261\ m^2\ g^{-1}$, 20–45 mesh) was chosen as the support because of its weak interaction with the sulfided phase which permits a better characterization. In a typical preparation of the K_2O–MoO_3–CoO/SiO_2 catalyst, the required quantities of K_2CO_3, $(NH_4)_6Mo_7O_{24}{\cdot}4H_2O$, and $Co(NO_3)_2{\cdot}6H_2O$ were dissolved in deionized water, to which ammonia was added until the precipitate was fully dissolved under stirring to yield an aqueous solution. Subsequently, SiO_2 was impregnated for 12 h, followed by drying and calcining at 400 °C for 4 h. The optimized amount of precursors was expressed as that of corresponding oxides according to [26]. For the sake of brevity, the samples thus prepared MoO_3/SiO_2 (25/100, wt/wt), MoO_3–CoO/SiO_2 (25–5/100, wt/wt), K_2O–MoO_3/SiO_2 (15–25/100, wt/wt), and K_2O–MoO_3–CoO/SiO_2 (15–25–5/100, wt/wt) were denoted as Mo/SiO_2, $MoCo/SiO_2$, KMo/SiO_2, and $KMoCo/SiO_2$, respectively. To have a better understanding of the effect of alkali metal, Li_2O–MoO_3/SiO_2 ($LiNO_3$ was used as the precursor) and Cs_2O–MoO_3/SiO_2 (Cs_2CO_3 was used as the precursor) were prepared according to the same molar ratio as K/Mo and denoted as $LiMo/SiO_2$ and $CsMo/SiO_2$, respectively.

2.2. Catalyst testing

The catalysts were tested by using a stainless-steel tubular fixed-bed flow microreactor. Before evaluation, 0.5 mL of oxidic catalysts were reduced with hydrogen at 420 °C for 4 h followed by sulfidation with the feedstock ($H_2S/H_2/CO = 2/1/1$, v/v) at 300 °C for 4 h. The feedstock of H_2S, CO, and H_2 was mixed into a cylinder beforehand, to which 2–3% (volume %) of N_2 was added as internal standard. The reactants and products were analyzed by using on-line gas chromatographs (GC) fitted with thermal conductivity detector (TCD), flame ionization detector (FID), flame photometric detector (FPD). N_2, CO, and CO_2 were analyzed by an on-line GC fitted with a TCD (a carbon molecular sieve column, 1.5 m × 8 mm). The hydrocarbons were analyzed by an on-line GC equipped with a FID (a Porapak Q column, 1.5 m × 8 mm). The sulfur-containing compounds were analyzed by an on-line GC fitted with a FPD (a HP-Plot/Q (19095P-Q04) capillary column, 30 m × 0.539 mm × 40.00 μm). Some products (thioethers) which could not be separated in the GC chromatograms were analyzed off-line with a Varian GC3900/SATURN 2100 w gas chromatograph–mass spectrometer (GC–MS). All lines from the reactor to the gas sampling valves were kept at ∼150 °C to prevent product condensation. All the activity and selectivity data were taken when the steady state was achieved.

2.3. Catalyst characterization

The sulfided catalysts were obtained from the tested samples. To avoid contacting air, the samples were cooled to room temperature in the atmosphere of argon and transferred into a glove box filled with Ar for grinding and tabletting. Then the ground and tabletted catalysts were kept in the sealed glass tubes or the cells for the physicochemical measurements.

The XRD patterns were obtained with a PANalytical X'pert PRO diffractometer with Cu Kα ($\lambda = 0.154$ nm) radiation. The tube voltage was 40 kV and the current was 30 mA. 2θ scans were taken from 5 to 70° with a step size of 0.008° and 10 s per step. The phase identification was performed by using X'Pert HighScore V1.0D software.

The ESR measurements were carried out on a Bruker EMX-10/12 EPR spectrometer. All ESR spectra were recorded with a microwave power of 54.1 mW, modulation amplitude of 6.00 G, modulation frequency of 100 kHz, and a time constant of 40.96 ms.

The XPS data were recorded on a PHI Quantum 2000X spectrometer operating with Al Kα (1486.6 eV) radiation source and the binding energies were referred to the carbon C1s peak ($E_b = 284.7$ eV). The XPS spectra were fitted by using Multipak V6.1A software based on the assumption that the peaks consist of a mixture of Lorentzian–Gaussian functions after a Shirley background subtraction, and that the peak area ratios and spin–orbit splitting for the doublet peak are fixed.

CO-TPD studies were performed in a conventional atmospheric pressure quartz flow reactor with He (40 mL/min) as the carrier gas. Typically, 100 mg of oxidic catalyst was filled and pretreated in the same way as we performed the catalyst evaluation, and finally cooled to 100 °C. In the subsequent steps, CO adsorption was performed at 100 °C for 30 min, and then purged with He until the baseline is steady. Then the TPD test was conducted by increasing the temperature to 700 °C at a heating rate of 10 °C/min.

3. Results and discussion

3.1. Catalytic performance for the synthesis of methanethiol

Table 1 shows the product distribution and the catalytic performance for the synthesis of methanethiol from H_2S-rich syngas at 300 °C. Catalysts without alkali metals exhibited a very low activity for the synthesis of methanethiol, COS being the dominant product (selectivity >94%), this feature was similar to the unmodified support. However, the CO conversion increased markedly over the potassium-promoted Mo-based catalysts. Meanwhile, the product distribution changed significantly. COS, CO_2, and CH_3SH became the main products, and the selectivity to CH_4 decreased. To have a better understanding of the role of potassium, we chose a less basic promoter (Li) and a more basic promoter (Cs) to modify the MoO_3/SiO_2 catalyst, respectively. The activity tests showed that the K-promoted catalyst exhibits the highest activity for the CH_3SH synthesis from H_2S-rich syngas (activity, $KMo/SiO_2 > CsMo/SiO_2 > LiMo/SiO_2$). The results of pathway study [3,21,22] showed that COS is a primary product, which is hydrogenated to CH_3SH and H_2O, and that most of CO_2 originates from water-gas shift (WGS) reaction. The hydrocarbons and thioethers originate from the hydrogena-

Table 1
Activity tests of the catalysts for the synthesis of methanethiol from H_2S-rich syngas[a]

Catalysts	Selectivity (%) (H_2O excluded)								Conversion of CO (%)
	CH_4	C_2H_4	C_2H_6	COS	CO_2	CH_3SH	CS_2	Thioethers[b]	
SiO_2	3.8	–	–	94.7	Trace	1.5	–	–	1.7
Mo/SiO_2	1.5	–	–	96.2	Trace	2.3	–	–	4.6
$MoCo/SiO_2$	2.7	Trace	–	94.6	Trace	2.7	–	–	8.3
$LiMo/SiO_2$	1.0	Trace	Trace	17.5	29.9	51.6	Trace	–	19.5
KMo/SiO_2	0.3	0.1	Trace	19.1	31.7	48.5	0.2	0.1	42.7
$CsMo/SiO_2$	0.3	0.1	Trace	23.2	33.0	43.3	0.1	Trace	38.9
$KMoCo/SiO_2$	0.6	0.1	Trace	16.6	36.6	45.7	0.3	0.1	62.4

[a] Reaction conditions: 300 °C, 0.2 MPa, 3000 h^{-1}, $CO/H_2/H_2S = 1/1/2$ (v/v).
[b] $CH_3SCH_3 + CH_3SSCH_3 + CH_3SSSCH_3$.

tion of CH_3SH. Therefore, the formation of large amounts of CO_2 shows that the addition of potassium also promotes the water-gas shift reaction. The data in Table 1 also show that the addition of cobalt to the KMo/SiO_2 catalyst increases the conversion of CO and the selectivity to CH_4, while it decreases the selectivities to COS and CH_3SH slightly. These observations can be attributed to the hydrogenation function of the cobalt promoter.

3.2. XRD characterization

Fig. 1 shows the XRD patterns of the support and the sulfided Mo-based catalysts (Mo/SiO_2, $MoCo/SiO_2$, KMo/SiO_2, and $KMoCo/SiO_2$). No evident diffraction peaks other than the broad peak at $2\theta = 21.4°$ for SiO_2 were detected on the potassium-free catalysts (Mo/SiO_2, and $MoCo/SiO_2$), indicating that Mo–S or Co–Mo–S species disperse well on the surface of SiO_2. However, the addition of K destroys the uniformity in distribution of the Mo or Co species, new peaks at $2\theta = 21.2$, 23.8, 29.7, 30.8, 43.5° for K_2SO_4 (PDF code: 00-003-0608), peaks at $2\theta = 16.7$, 19.0, 24.8° for $K_2MoO_2S_2$ (PDF code: 00-023-1355), and peaks at $2\theta = 9.3$, 26.5, 28.0, 41.3° for S_6 (PDF code: 01-072-2402) were detected. The atomic ratio of K: Mo on the K_2O–MoO_3/SiO_2 (15–25/100, wt/wt) and K_2O–MoO_3–CoO/SiO_2 (15–25–5/100, wt/wt) catalysts is as high as 1.8: 1, thus the K–Mo interaction leads to the formation of KMo-containing bulk oxide phases (e.g., K_2MoO_4) [27]. Therefore, on the sulfided KMo/SiO_2 and $KMoCo/SiO_2$ catalysts, $K_2MoO_2S_2$ can be considered as the partial exchange product of K_2MoO_4 with sulfur. It has been claimed that some K–Mo–S and/or K–Mo–S–O species are formed after sulfidation of the oxidized catalyst precursors, which are correlated with active sites for mixed alcohol synthesis [16–18]. It is interesting that cyclic hexaatomic sulfur (S_6), which is a very active sulfur species, forms over the KMo/SiO_2 and $KMoCo/SiO_2$ catalysts during sulfidation. TPS characterizations [28] have reported that elemental sulfur was formed in the sulfidation of molybdenum catalysts, which was referred to be non-stoichiometric sulfur (S_x) by Janssens et al. [29]. On the sulfided vanadium-based catalysts supported on TiO_2 and Al_2O_3, Mul et al. further [3] proposed that S_x plays a role in the formation of carbonyl sulfide (COS) and active H:

$$H_2S \rightleftharpoons 2H + S_x$$

$$CO + S_x \rightleftharpoons COS$$

The resulting COS is hydrogenated to CH_3SH. Therefore, such low valent sulfur species may be related to the CO conversion and the formation of CH_3SH.

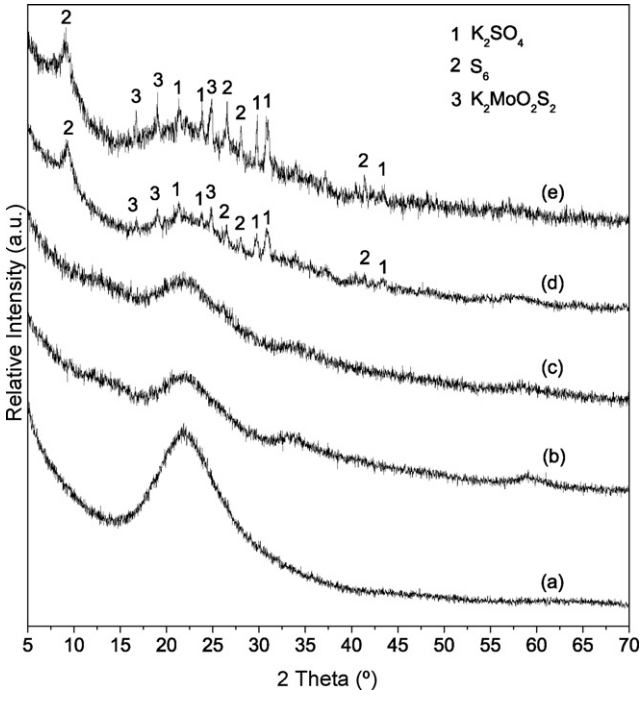

Fig. 1. X-ray diffraction patterns of the sulfided catalysts: (a) SiO_2, (b) Mo/SiO_2, (c) $MoCo/SiO_2$, (d) KMo/SiO_2, and (e) $KMoCo/SiO_2$.

3.3. CO-TPD studies

Fig. 2 shows the CO-TPD curves of the sulfided catalyst. Two types of CO desorption peaks were observed. The desorption peaks at low temperature (340–380 °C) are attributed to the non-dissociative adsorption of CO on the so-called coordinatively unsaturated molybdenum sites (Mo(CUS)), while the peaks at high temperature (510–580 °C) may be assigned to the dissociative adsortption controlled by kinetics or the sulfur-containing compounds [16,30,31]. The high temperature desorption peaks

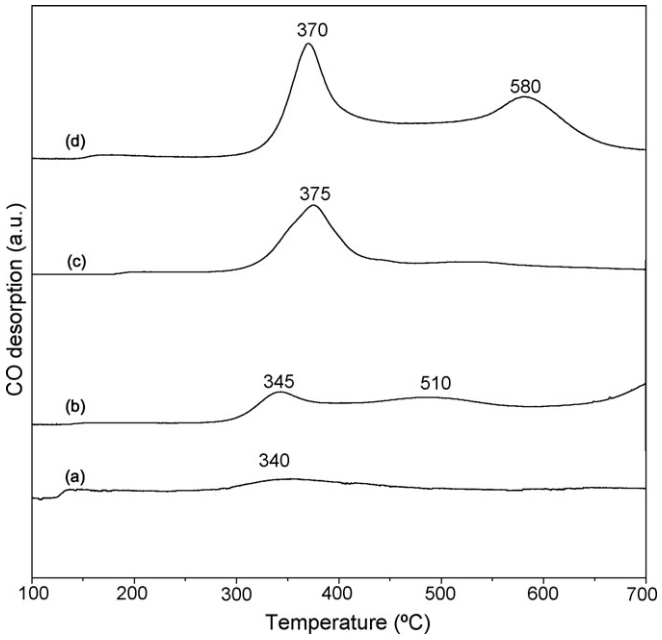

Fig. 2. CO-TPD curves of the sulfided catalysts: (a) Mo/SiO_2, (b) $MoCo/SiO_2$, (c) KMo/SiO_2, and (d) $KMoCo/SiO_2$.

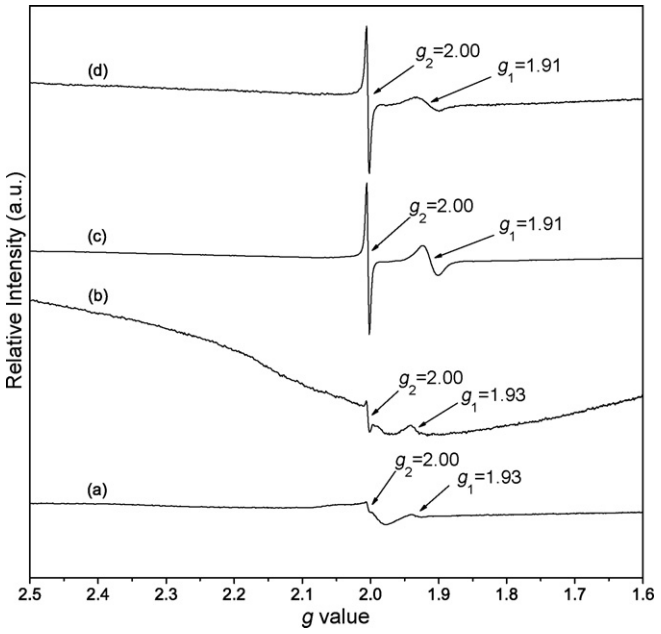

Fig. 3. ESR spectra of the sulfided catalysts: (a) Mo/SiO_2, (b) $MoCo/SiO_2$, (c) KMo/SiO_2, and (d) $KMoCo/SiO_2$.

were only observed in the Co-doped catalysts. Generally, the dissociative adsorption of CO leads to the formation of hydrocarbons [32]. This effect may explain that the selectivities to C_{1-2} on $KMoCo/SiO_2$ are higher than those on KMo/SiO_2.

Potassium species themselves do not provide sites for CO adsorption. The addition of potassium promotes the adsorption of CO on the KMo/SiO_2 and $KMoCo/SiO_2$ catalysts, this effect is better interpreted in terms of electronic effects [11,13,33]: the potassium considered as a base interacts with the transition-metal components, transferring electrons to the metallic phase, thus lowering the metal work function and results in increasing the adsorption of electron-acceptor molecules such as CO and weakening the C–O bonds. The doping with potassium not only promotes the adsorption of CO but also increases the coordinatively unsaturated molybdenum sites, which may be closely related to the synthesis of CH_3SH. Tatsumi et al. [10] suggested that the potassium increases the active sites for the alcohol formation by retarding the reduction of Mo. Therefore, it is essential to deposit a basic additive on the Mo/SiO_2 catalyst for the synthesis of CH_3SH.

3.4. ESR characterization

Fig. 3 presents the ESR spectra of the sulfided Mo-based catalysts. Two signals (g_1 and g_2) were detected. The resonant signal of g_1 is ascribed to the oxo-Mo^{5+} species, which is difficult to be sulfided because of its strong interaction with SiO_2 [34,35]. Interestingly, a shift of the signal of oxo-Mo^{5+} to higher fields after the addition of potassium is observed (g_1 equals 1.93 on Mo/SiO_2 and $MoCo/SiO_2$, but 1.91 on KMo/SiO_2 and $KMoCo/SiO_2$). It is probable that the interaction between potassium and molybdenum decreases the number of O^{2-} ligands. Another signal at $g_2 = 2.00$ is an overlapping signal, which characterizes the co-existence of oxysulfo-Mo^{5+} species and trace amounts of paramagnetic sulfur species [36–39]. Due to the partial exchange of oxygen for sulfur and the redox process, Mo(VI) oxidic species give rise to oxysulfo-Mo^{5+} species ($O_xMo^{5+}S_y$) in the $H_2S/H_2/CO$ atmosphere at 300 °C. The paramagnetic sulfur species are attributed to disulfur radicals (S_2^-) or polysulfur species (S_x^-) produced during the adsorption of trace amounts of H_2S [36,40–43]. Kolosov [36] et al. reported that the S_3^- anion radical is still stable in the presence of other molecules such as O_2, H_2O, NH_3, SO_2, C_3H_6, and H_2S at room temperature. Moreover, the signals of g_2 on the potassium-containing catalysts (KMo/SiO_2 and $KMoCo/SiO_2$) are more axially symmetric than that on the potassium-free catalysts (Mo/SiO_2 and $MoCo/SiO_2$), indicating that the corresponding species of oxysulfo-Mo^{5+} are more stable. Furthermore, the intensity of g_2 is much larger than that of g_1 over all four Mo-based catalysts, indicating that most Mo^{5+} ions are located in an oxysulfo-surrounding. ESR experiments indicate that potassium stabilizes the Mo species in a +5 valence state after sulfidation, which is consistent with the result reported in [44].

Compared with Fig. 3(c) with (d), the intensity of oxo-Mo^{5+} on KMo/SiO_2 is bigger than that on $KMoCo/SiO_2$, indicating that cobalt promotes the sulfidation of oxo-Mo^{5+} species.

3.5. XPS characterization

The Mo (3d) XPS spectra of the sulfided catalysts are presented in Fig. 4. The binding energies of $Mo3d_{5/2}$ at ~229, ~231, and ~233 eV are assigned to the oxidation states of +4, +5, and +6, respectively. The shoulder at binding energy of 226.60 eV is ascribed to the S2s peak [45,46]. The contribution of S2s level is subtracted and the fitting results are shown in Table 2. The data reveal that the addition of potassium or cobalt influ-

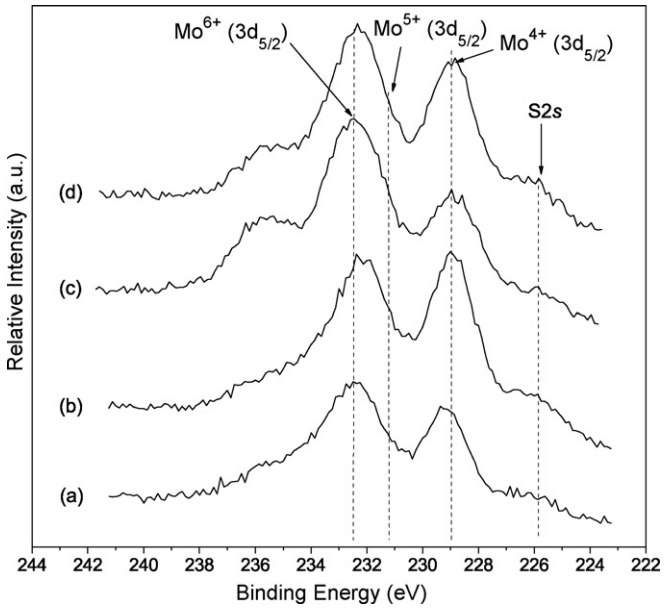

Fig. 4. Mo (3d) XPS spectra of the sulfided catalysts: (a) Mo/SiO_2, (b) $MoCo/SiO_2$, (c) KMo/SiO_2, and (d) $KMoCo/SiO_2$.

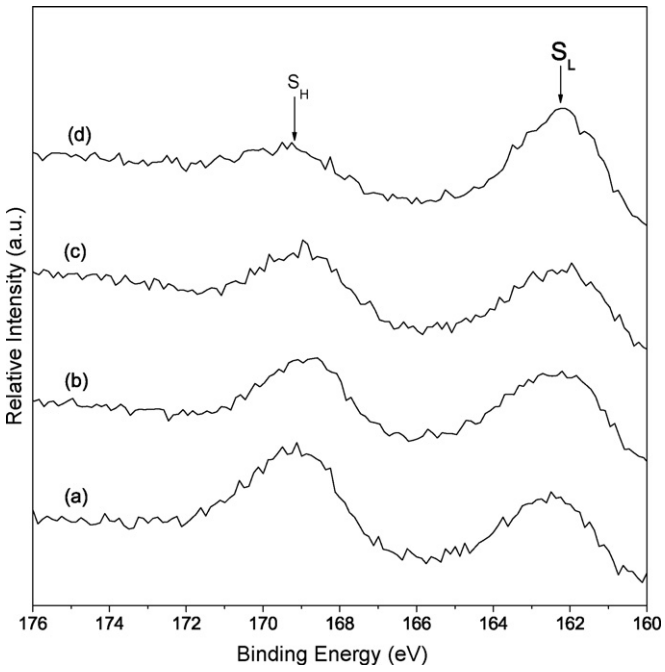

Fig. 5. S (2p) XPS spectra of the sulfided catalysts: (a) Mo/SiO_2, (b) $MoCo/SiO_2$, (c) KMo/SiO_2, and (d) $KMoCo/SiO_2$.

ences the balance among the three Mo oxidation states. The addition of potassium leads to the increase of Mo^{5+} concentration and a simultaneous decrease of Mo^{4+} concentration, and results in the ratio of Mo^{5+}/Mo^{4+} on the potassium-free catalyst is lower than that on the potassium-containing catalyst. However, the effect of cobalt on the Mo species is smaller than that of potassium. These features are in agreement with the results of ESR characterizations. Associating the catalytic activity (Table 1) and the results of ESR and XPS characterizations, Co does not change the intrinsic activity of Mo, the promoting effect of Co on the activity for the synthesis of CH_3SH is possible that Co combines with Mo–S species to form the so-called "Co–Mo–S" phase which favors the hydrogenation reactions [41] or Co itself provides the active sites for CH_3SH synthesis. It is generally believed that Mo(VI) oxidic species exist predominately in octahedral and tetrahedral coordination, and that the tetrahedral Mo(VI) is less susceptible to reduction and sulfidation than octahedral Mo(VI) [47,48]. Due to the interaction between the potassium promoter and the Mo components, part of the octahedral Mo(VI) species transforms into tetrahedral Mo(VI) species [48]. Thus the reducibility of Mo species is diminished in the presence of potassium, as a result, the Mo^{5+} species are stabilized on the KMo/SiO_2 and $KMoCo/SiO_2$ catalysts after sulfidation, while the Mo^{4+} species are preferable on the Mo/SiO_2 and $MoCo/SiO_2$ catalysts. The results are in agreement with those reported by Watson and Ozkan [44] and Kantschewa et al. [49]. Some authors [27] pointed out that the basic promoters inhibit the reduction of MoO_3 by strengthening the Mo–O bonds and increasing the reduction activation energies.

Fig. 5 shows the S (2p) XPS spectra of the sulfided catalysts. The sulfur species at low binding energy are attributed to elemental sulfur (164.0 eV), S^{2-} (162.0 eV), S_2^{2-} (162.5 eV), oxysulfides (162.3–163.2 eV), and polysulfides (162.9–164.4 eV) [42,50]. The sulfur species at high binding energy may be assigned to SO_4^{2-} species (169.1 eV) [51], which result from the oxidation of the part of the adsorbed H_2S or the low valent sulfur because the oxidizing agents such as H_2O and CO_2 are present in the reaction system [39,52]. For the sake of brevity, two forms of sulfur species, i.e., "low oxidation state sulfur species" and "high oxidation state sulfur species" are defined, which are labeled as "S_L" and "S_H" in Fig. 5, respectively. The fitting results are presented in Table 3.

As shown in Table 3, the S_L/S_H ratio increases with the addition of cobalt and/or potassium. The ability of low valent sulfur ions, both S^{2-} and S_2^{2-}, on MoS_2-based catalysts to

Table 2
The fitting results of Mo (3d) XPS spectra of the tested catalysts

Catalyst	Binding energy of $Mo3d_{5/2}$ (eV)			Concentration (%)			Ratio of Mo^{5+}/Mo^{4+}
	Mo^{4+}	Mo^{5+}	Mo^{6+}	Mo^{4+}	Mo^{5+}	Mo^{6+}	
Mo/SiO_2	229.1	231.2	232.7	69.1	10.5	20.4	0.2
$MoCo/SiO_2$	228.9	230.9	232.4	61.1	12.1	26.8	0.2
KMo/SiO_2	228.7	231.4	232.7	44.0	22.3	33.7	0.5
$KMoCo/SiO_2$	228.5	229.8	232.7	41.6	21.8	36.6	0.5

Table 3
The fitting results of S (2p) XPS spectra of the tested catalysts

Catalyst	Concentration (%)		Ratio of S_L/S_H
	S_L[a]	S_H[a]	
Mo/SiO_2	44.0	56.0	0.8
$MoCo/SiO_2$	51.9	48.1	1.1
KMo/SiO_2	59.2	40.8	1.5
$KMoCo/SiO_2$	70.3	29.7	2.4

[a] S_L, low oxidation state sulfur species; S_H, high oxidation state sulfur species.

activate H_2 has been proved. The S_L/S_H ratio is higher over the $KMoCo/SiO_2$ catalyst than that over the KMo/SiO_2 catalyst, which can be related to the higher selectivities to hydrocarbons and thioethers on $KMoCo/SiO_2$ than those on KMo/SiO_2. Two mechanisms for activating H_2 have been suggested. One is homolytical cleavage over S_2^{2-} [53–55]:

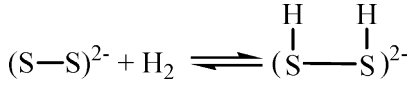

the other is heterolytical cleavage over Mo–S bond:

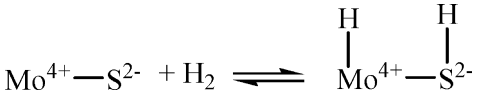

Oxidic Mo(VI) species are reduced and sulfided to Mo^{5+} and Mo^{4+} species in the atmosphere of $H_2S/H_2/CO$ at 300 °C, thus the Mo–S and Mo–Mo coordination number for the sulfided catalysts decreases markedly and the surface reconstruction takes place, which may lead to the formation of "residual" sulfur species and the increase of coordinatively unsaturated molybdenum sites [10,56]. Muijsers et al. [37] and Weber et al. [38] gave detailed evidence for the co-existence of bridging $(S–S)^{2-}$ ligands and Mo^{5+} centers in sulfided Mo species. The increase of the oxysulfo-Mo^{5+} concentration will decrease the content of S^{2-} species but simultaneously increase that of S_2^{2-} and S_x species. Overall, the low valent sulfur species increase with the addition of potassium, which may favor the synthesis of methanethiol.

3.6. Proposed mechanism for the CH_3SH synthesis

It is well known that methanol is formed from the reaction of syngas (containing no H_2S or very low content of H_2S) over the catalysts comprising basic components (B) and hydrogenation components (M). The role of basic additives is supposed to stabilize the metal cations, which favor CO insertion into a metal cation hydride bond (M–H), thus the resulting formyl species (M–COH) is hydrogenated to methanol [57]. Others suggested that basic promoter play a role in keeping the oxygen anions at the metal surface, with which the absorbed CO react to generate the formate intermediate (M–COO), which subsequently hydrogenated to CH_3OH [58]. Klier et al. [12,59] proposed a "bifunctional" model for the alkali-promoted MoS_2 catalysts: the alkali metal favors the non-dissociative adsorption of CO and MoS_2 activates the H_2. Recent results reported by Gotti and Prins [60,61] and Jerdev et al. [62] show that the basic metal oxides serve as one part of the active components, with which CO reacts to produce formate (B–COOH), then the resulting formate species react with hydrogen atoms supplied by the hydrogenation components to form methanol. In this study, although CH_3OH could be formed in the reaction of H_2 and CO, the CH_3SH is cannot be formed by the reaction of CH_3OH and H_2S since no methanol is detected in the products.

Based on different product distribution and catalysts, two mechanisms for the synthesis of methanethiol from $CO/H_2/H_2S$ mixtures have been proposed. Barrault et al. (using sulfided $K–WO_3/Al_2O_3$) [22] and Mul et al. [3] (using sulfided V_2O_5/TiO_2 and V_2O_5/Al_2O_3) proposed a reaction pathway for the formation of CH_3SH from the hydrogenation of carbonyl sulfide (COS), which proceeds via a surface thioformic ($HOCS_{ads}$) and a subsequent surface methylthiolate (CH_3S_{ads}) intermediate [21]. However, based on the facts that the product distribution showed an approximate Anderson–Schulz–Flory character and no COS was detected, Zhang et al. [24] proposed a modified mechanism of the F-T process incorporating a reaction of a C_1 intermediate with a surface –SH group for the synthesis of CH_3SH over unmodified α-Al_2O_3 catalysts. In this study, CH_3SH, COS, and CO_2 are the predominant products, suggesting that the synthesis of CH_3SH over K-promoted Mo/SiO_2 catalysts proceed via the former reaction pathway.

It is essential to deposit a basic additive on the Mo/SiO_2 catalyst for the synthesis of CH_3SH. For the bi-component KMo/SiO_2 catalyst and tri-component $KMoCo/SiO_2$ catalyst, since the high content of H_2S in syngas could supply enough S^{2-} and/or SH^- groups, the function of potassium thus could be suggested to furnish K–S and/or K–SH bonds, into which the non-dissociative adsorption of CO can insert. The formed carbonyl sulfide (COS_{ads}) and/or thioformate ($HOCS_{ads}$) can then be hydrogenated to methylthiolate (CH_3S_{ads}) by the spillover of active hydrogen atoms on the sulfided Mo or Co–Mo components (Mo^{4+}–S^{2-}, Co–Mo–S, S_2^{2-}, or S_x species), the subsequent hydrogenation of methylthiolate produces CH_3SH. Thus the base-doped Mo-based catalysts are the bifunctional catalysts. Total reactions are as follows:

$$CO + H_2S \leftrightarrow COS + H_2 \quad (1)$$

$$COS + 3H_2 \leftrightarrow CH_3SH + H_2O \quad (2)$$

Reaction (1) can easily take place over the unmodified SiO_2 or the transition-metal sulfides, however, the equilibrium constant of reaction (1) is very small ($K_p = 0.04$ at 300 °C calculated from $\ln K_p = -\Delta_r G(T)/RT$, where the $\Delta_r G(T)$ is the Gibbs energy change at 300 °C and R is the universal gas constant) [63,64]. Reaction (2) is the rate-determining step for the synthesis of CH_3SH [22]. The presence of potassium favors the activations of CO and COS on the surface of the catalysts (Fig. 2), which favors the subsequent hydrogenation to CH_3SH. These features explain the facts that the COS dominates the products and CO conversion is low over the potassium-free catalysts (Mo/SiO_2 and $MoCo/SiO_2$). The more basic additives favor the formation of COS but their stronger nucleophilic character makes the thioformate species more stable, which reduces the hydrogenation of

COS to CH_3SH. While the less basic additives favor the hydrogenation of COS but their weaker nucleophilic character are not favorable to form COS. Both cases do not favor the formation of CH_3SH (as shown in Table 1). These observations are similar to those reported by Gotti and Prins [60,61]. Due to the interaction between K and Mo (Fig. 1), K can be considered as one part of the active components on the sulfided K–Mo/SiO_2 and K–Mo–Co/SiO_2 for the synthesis of CH_3SH. The active phases may be the K–Mo–(Co)–S and/or K–Mo–(Co)–S–O species.

After the formation of H_2O, the WGS reaction will take place:

$$CO + H_2O \leftrightarrow CO_2 + H_2 \quad (3)$$

Hou et al. [65] proposed that the WGS reaction mechanism involves a Mo^{5+}/Mo^{4+} redox cycle over the molybdenum sulfide-based catalyst. Therefore higher concentration of Mo^{5+} species and higher ratio of Mo^{5+}/Mo^{4+} favor the WGS reaction (Figs. 3 and 4, Table 2). The addition of potassium also promotes the WGS reaction (Table 1). Thus, two competing reactions, i.e., the reaction between H_2S and CO and the reaction between H_2O and CO, will determine the product distribution. In this study, on the one hand the high H_2S concentration is present in reaction system; on the other hand the sulfur is more nucleophilic than oxygen, so CH_3SH is more dominant than CO_2 in the product. If a high concentration of H_2O existed in the reaction system (for example, when H_2O is injected into the reactor), CO_2 should be more dominant than CH_3SH. These expectations have been supported by the results of Mul et al. [3]. Surely the product distribution is also affected by other factors such as the rate of each elementary steps, temperature, pressure, and dynamics control.

4. Conclusions

In this paper, the synthesis of methanethiol from H_2S-rich syngas over Mo-based catalysts was investigated. It is shown that potassium-promoted Mo-based catalysts exhibit a high activity for the CH_3SH synthesis. The incorporation of cobalt into the K–Mo/SiO_2 catalyst increases the catalytic activity, but slightly decreases the selectivity to methanethiol. XRD characterization shows that the interaction between K and Mo occurs after the addition of relatively high potassium content, leading to the formation of KMo-containing compounds. CO-TPD studies show that the deposit of potassium increases the number of active sites for the CH_3SH synthesis. ESR characterization shows that the potassium stabilizes and increases Mo^{5+} species after sulfidation. XPS analysis indicates that the potassium influences the balance between the Mo species and S species in the sulfided state. The increase of the ratios of Mo^{5+}/Mo^{4+} and low valent sulfur/high valent sulfur favors the synthesis of CH_3SH from the H_2S-rich syngas, however, it also promotes the water-gas shift reaction. Potassium serves as one part of the active components on the sulfided K–Mo or K–Mo–Co catalysts, which may benefit the insertion of CO to generate the intermediates for the CH_3SH synthesis. The mechanism suggests that water-gas shift reaction, co-existing with the reaction of methanethiol synthesis, reduces the atom utilization of carbon to a certain extent.

Acknowledgement

The authors gratefully acknowledge Degussa GmbH (Germany) for the financial support.

Appendix A. Supplementary data

Supplementary data associated with this article can be found, in the online version, at doi:10.1016/j.molcata.2007.12.014.

References

[1] J. Sauer, W. Boeck, L. von Hippel, W. Burkhardt, S. Rautenberg, D. Arntz, W. Hofen, US Patent 5 582 219 (1998), to Degussa Aktiengesellschaft.
[2] H. Ponceblance, F. Tamburro, US Patent 5 847 223 (1998), to Rhone-Poulenc Nurtrition Animale.
[3] G. Mul, I.E. Wachs, A.S. Hirschon, Catal. Today 78 (2003) 327.
[4] G.J. Quarderer, K.A. Cochran, EP Patent 0 119 609 (1984), to Dow Chemical Company.
[5] D.B. Duane, H.P. William, D.G. Lawrence, EP Patent 0 085 191 (1983), to Union Carbide Corp.
[6] M.M. Conway, C.B. Murchison, R.R. Steven, US Patent 4 675 344 (1987), to Dow Chemical Company.
[7] R.R. Stevens, US Patent 4 752 622 (1988), to Dow Chemical Company.
[8] T. Tatsumi, A. Muramatsu, H. Tominaga, J. Catal. 101 (1986) 553.
[9] X. Youchang, B.M. Nassa, G.A. Somorjai, Appl. Catal. 27 (1986) 233.
[10] T. Tatsumi, A. Muramatsu, K. Yokota, H. Tominaga, J. Catal. 115 (1989) 388.
[11] H. Praliaud, J.A. Dalmon, C. Mirodatos, A. Martin, J. Catal. 97 (1986) 344.
[12] J.G. Santiesteban, C.E. Bogdan, R.G. Herman, K. Klier, in: M.J. Phillips, M. Ternan (Eds.), Proceedings of 9th ICC, Calgary, Ottawa, 1988, p. 561.
[13] Y. Avila, C. Kappenstein, S. Pronier, J. Barrault, Appl. Catal. A 132 (1995) 97.
[14] X.D. Xu, E.B.M. Doesburg, J.J.F. Scholten, Catal. Today 2 (1986) 125.
[15] H.C. Woo, I.S. Nam, J.S. Lee, J.S. Chung, Y.G. Kim, J. Catal. 142 (1993) 672.
[16] M. Jiang, G.Z. Bian, Y.L. Fu, J. Catal. 146 (1994) 144.
[17] G.Z. Bian, L. Fan, Y.L. Fu, K. Fujimoto, Appl. Catal. A 170 (1998) 255.
[18] N. Koizumi, G.Z. Bian, K. Murai, T. Ozaki, M. Yamada, J. Mol. Catal. A 207 (2004) 173.
[19] B. Buchholz, US Patent 4 410 731 (1983), to Pennwalt Corporation.
[20] Y.Q. Yang, Y.Z. Yuan, S.J. Dai, B. Wang, H.B. Zhang, Catal. Lett. 54 (1998) 65.
[21] D.D. Beck, J.M. White, C.T. Ratcliffe, J. Phys. Chem. 90 (1986) 3123.
[22] J. Barrault, M. Boulinguiez, C. Forquy, R. Maurel, Appl. Catal. 33 (1987) 309.
[23] B. Zhang, S.H. Taylor, G.J. Hutchings, Catal. Lett. 91 (2003) 181.
[24] B. Zhang, S.H. Taylor, G.J. Hutchings, New J. Chem. 28 (2004) 471.
[25] Y.Q. Yang, S.J. Dai, Y.Z. Yuan, R.C. Lin, D.L. Tang, H.B. Zhang, Appl. Catal. A 192 (2000) 175.
[26] Y.Q. Yang, H. Yang, Q. Wang, L.J. Yu, C. Wang, S.J. Dai, Y.Z. Yuan, Catal. Lett. 74 (2001) 221.
[27] K. Chen, S. Xie, A.T. Bell, E. Iglesia, J. Catal. 195 (2000) 244.
[28] P. Arnoldy, J.A.M. van den Heijkant, G.D. de Bok, J.A. Moulijn, J. Catal. 92 (1985) 35.
[29] J.P. Janssens, A.D. van Langeveld, J.A. Moulijn, Appl. Catal. A 179 (1999) 229.
[30] J. Valyon, W.K. Hall, J. Catal. 84 (1983) 216.
[31] M.I. Zaki, B. Viehaber, H. Knözinger, J. Phys. Chem. 90 (1986) 3176.
[32] J.A. Rabo, A.P. Risch, M.L. Poutsma, J. Catal. 53 (1978) 295.
[33] D.B. Compton, T.W. Root, J. Catal. 137 (1992) 199.
[34] A.J.A. Konings, V.A.M. Dooren, D.C. Koningsberger, V.H.J. de Beer, A.L. Farragher, G.C.A. Schuit, J. Catal. 54 (1978) 1.
[35] A.J.A. Konings, W.L.J. Brentjens, D.C. Koningsberger, V.H.J. de Beer, J. Catal. 67 (1981) 145.

[36] A.K. Kolosov, V.A. Shvets, N.D. Chuvylkin, V.B. Kazansky, J. Catal. 55 (1978) 394.
[37] J.C. Muijsers, Th. Weber, R.M. van Hardeveld, H.W. Zandbergen, J.W. Niemantsverdriet, J. Catal. 157 (1995) 698.
[38] Th. Weber, J.C. Muijsers, J.H.M.C. van Wolput, J.W. Niemantsverdriet, J. Phys. Chem. 100 (1996) 14144.
[39] D. Nikolova, R. Edreva-Kardjieva, G. Gouliev, T. Grozeva, P. Tzvetkov, Appl. Catal. A 297 (2006) 135.
[40] K.C. Khulbe, R.S. Mann, J. Catal. 51 (1978) 364.
[41] E.G. Derouane, E. Pedersen, B.S. Clausen, Z. Gabelica, R. Candia, H. Topsøe, J. Catal. 99 (1986) 253.
[42] M. Steins, P. Koopman, B. Nieuwenhuijse, P. Mars, J. Catal. 42 (1976) 96.
[43] B.G. Silbernagel, T.A. Pecoraro, R.R. Chianelli, J. Catal. 78 (1982) 380.
[44] R.B. Watson, U.S. Ozkan, J. Mol. Catal. A 194 (2003) 115.
[45] M.A. Baker, R. Gilmore, C. Lenardi, W. Gissler, Appl. Surf. Sci. 150 (1999) 255.
[46] N.M.D. Brown, N. Cui, A. McKinley, Appl. Surf. Sci. 134 (1998) 11.
[47] S.J. DeCanio, M.C. Cataldo, E.C. DeCanio, D.A. Storm, J. Catal. 119 (1989) 256.
[48] L. Feng, X. Li, D.B. Dadyburjor, E.L. Kugler, J. Catal. 190 (2000) 1.
[49] M. Kantschewa, F. Delannay, H. Jeziorowski, E. Delgado, S. Eder, G. Ertl, H. Knözinger, J. Catal. 87 (1984) 482.
[50] P.A. Spevack, S. McIntyre, Appl. Catal. 64 (1990) 191.
[51] C.D. Wagner, J.A. Taylor, J. Electron Spectrosc. Relat. Phenom. 28 (1982) 211.
[52] P. Gajardo, A. Mathieux, P. Grange, B. Delmon, Appl. Catal. 3 (1982) 347.
[53] J.A. Spirko, M.L. Neiman, A.M. Oelker, K. Klier, Surf. Sci. 572 (2004) 191.
[54] A.N. Startsev, I.I. Zakharov, V.N. Parmon, J. Mol. Catal. A 192 (2003) 113.
[55] L.S. Byskov, M. Bollinger, J.K. Nørskov, B.S. Clausen, H. Topsøe, J. Mol. Catal. A 163 (2000) 117.
[56] G.Z. Bian, Y.L. Fu, M. Yamada, Appl. Catal. A 144 (1996) 79.
[57] J. Nakamura, I. Nakamura, T. Uchijima, Y. Kanai, T. Watanabe, M. Saito, T. Fujitani, Catal. Lett. 31 (1995) 325.
[58] K.C. Waugh, Catal. Today 18 (1993) 147.
[59] K. Klier, R.G. Herman, J.G. Nunam, K.J. Smith, C.E. Bogdan, C.W. Young, J.G. Santiesteban, Stud. Surf. Sci. Catal. 36 (1988) 109.
[60] A. Gotti, R. Prins, J. Catal. 175 (1998) 302.
[61] A. Gotti, R. Prins, J. Catal. 178 (1998) 511.
[62] D.I. Jerdev, R. Prins, B.E. Koel, J. Phys. Chem. B 108 (2004) 14417.
[63] K. Fukuda, M. Dokiya, T. Kemeya, Y. Kotera, J. Catal. 49 (1973) 379.
[64] F. Faraji, I. Safarik, O.P. Strausz, M.E. Torres, E. Yildirim, Ind. Eng. Chem. Res. 35 (1996) 3854.
[65] P. Hou, D. Meeker, H. Wise, J. Catal. 80 (1983) 280.